©2005 IEEE. Personal use of this material is permitted. However, permission to reprint/republish this material for advertising or promotional purposes or for creating new collective works for resale or redistribution to servers or lists, or to reuse any copyrighted component of this work in other works must be obtained from the IEEE.

Learning and Detecting Activities from Movement Trajectories Using the Hierarchical Hidden Markov Model

Nam T. Nguyen, Dinh Q. Phung, Svetha Venkatesh
Department of Computing
Curtin University of Technology
GPO Box U 1987, Perth, Western Australia
{nguyentn,phungquo,svetha}@cs.curtin.edu.au

Hung Bui Artificial Intelligence Center SRI International 333 Ravenswood Ave, Menlo Park CA 94025, USA, bui@ai.sri.com

Abstract

Directly modeling the inherent hierarchy and shared structures of human behaviors, we present an application of the hierarchical hidden Markov model (HHMM) for the problem of activity recognition. We argue that to robustly model and recognize complex human activities, it is crucial to exploit both the natural hierarchical decomposition and shared semantics embedded in the movement trajectories. To this end, we propose the use of the HHMM, a rich stochastic model that has been recently extended to handle shared structures, for representing and recognizing a set of complex indoor activities. Furthermore, in the need of real-time recognition, we propose a Rao-Blackwellised particle filter (RBPF) that efficiently computes the filtering distribution at a constant time complexity for each new observation arrival. The main contributions of this paper lie in the application of the sharedstructure HHMM, the estimation of the model's parameters at all levels simultaneously, and a construction of an RBPF approximate inference scheme. The experimental results in a real-world environment have confirmed our belief that directly modeling shared structures not only reduces computational cost, but also improves recognition accuracy when compared with the tree HHMM and the flat HMM.

1 Introduction

Building intelligent systems in smart environments is the goal of much research [1, 6, 10, 11, 12, 13]. In most of these systems, modeling and recognizing activities, especially complex activities, is a crucial problem. Although activities can be inferred from a wide range of data given by sensors that pervade the environment, we restrict this discussion to data acquired through video cameras, that is, trajectories. When a person executes several actions in an environment, these actions can often be broken into smaller components. For example, the action of "making breakfast" involves a sequence of subtasks: (a) go_to_cupboard, (b) go_to_fridge, and (c) go_to_dining_table. Another action, such as "cooking dinner", may involve go_to_fridge, go_to_stove, and go_to_dining_table. Thus, not only do normal activities have a natural hierarchy, they also have shared subactions.

The hidden Markov model (HMM) and some of its extensions, such as the couple hidden Markov model (CHMM) or the variable length Markov model (VLMM), are efficient for representing and recognizing simple activities [5, 9, 15]. However, these flat models are inadequate to model complex activities because they cannot characterize the hierarchic and shared structure naturally embedded in the activities. Earlier approaches to tackling this problem include the layered hidden Markov model (LHMM) [14], stochastic context free grammar (SCFG) [17], the abstract hidden Markov model (AHMM) [4], and the hierarchical hidden Markov model (HHMM) [8, 3].

In [14], Oliver et al. use the LHMM for recognizing highlevel activities based on real-time streams of signals from multiple sources of sensors. The activities are classified level by level using the HMM. The inference influence in the activity hierarchy is one way: from low level to high level. Ivanov and Bobick [11] propose a two-stage algorithm for behavior recognition. The primitive behaviors are detected at low level using the basic HMM. Then, the system uses an SCFG to recognize high-level behaviors. These approaches, however, do not offer an integrated method for inferring behaviors all the way from low level to high level. A fully integrated system for modeling and detecting both high-level and low-level behaviors is proposed by Nguyen et al. [13]. The system uses the abstract hidden Markov memory model (AHMEM) [2] to model the behavior hierarchy. Although the system is expressive in representing high-level behaviors, it is limited in learning the behaviors' parameters.

Osentoski *et al.* [16] introduce a system using the AHMM [4] for representing the behaviors. Parameters for the model can be learned from labeled or unlabeled data using the expectation maximization (EM) algorithm, in which the inference at the E-step is achieved by the junction tree algorithm. However, when the depth of the model increases, this method can quickly become intractable because of the blow up in the maximum clique size. Another limitation of this system is that special landmarks are not taken into account, thus limiting the expressiveness of the behavior hierarchy. Liao *et al.* [12] propose a surveillance system using GPS sensors to infer a user's daily activities in a large and complex environment. The AHMM is used to represent the activity hierarchy, which has the following levels: (1) user's goals, (2)

trip segments (start locations, stop locations, and modes of transportation), and (3) user's locations and velocities. The EM algorithm is used to learn the user's goals and important locations from unlabeled data. The parameters of the hierarchical activity are then estimated using the Monte Carlo EM method [19]. It is not clear how the accuracy of this method would degrade when the complexity of the model and the observation length increase.

This paper aims to use the HHMM, in particular its recent extension [3] that allows for shared structures, for tackling two issues: (a) modeling and learning complex behaviors from human indoor trajectories and (b) recognizing the behaviors from new trajectories. We argue that to build robust and scalable behavior recognition systems, it is crucial to model not only the natural hierarchical decomposition in the movement trajectories, but also the inherent shared structure embedded in the hierarchy. The shared structures can also be duplicated and represented using a tree-like structure as in [8], but as empirically shown in this paper, our proposed shared structure model not only saves computational time but is also superior in the recognition accuracy when compared against the tree HHMM and the flat HHM. In addition, using the HHMM to model activities allows us to incorporate prior knowledge about the structure of the behavioral hierarchy. In the need of real-time inference, the Rao-Blackwellised particle filter (RBPF) used in the dynamic Bayesian network (DBN) [7] and especially in the AHMM [4] is adapted to provide an efficient approximate inference method. Empirical results demonstrating the advantages of this RBPF scheme over the exact inference method are also reported.

The novelty of this paper is threefold. (1) To the best of our knowledge, we are the first to apply the HHMM with shared structures to the problem of activity recognition in a real environment and we demonstrate its superiority over the flat HMM and tree HHMM. (2) We estimate the model parameters in an integrated way, as compared with other approaches that employ level-by-level parameter estimation [14, 11]. Our learning framework goes beyond the work of Osentoski et al. [16] and Liao et al. [12] by using an efficient, scalable, and exact algorithm for the problem of learning the model's parameters, as opposed to the use of the EM and junction tree inference algorithms in [16] or the Monte Carlo EM algorithm in [12]. (3) We adapt the RBPF algorithm to the HHMM and compare the results with an exact inference algorithm, demonstrating the usefulness of this approximate inference scheme.

2 Hierarchical Hidden Markov Models

The HHMM, first introduced in [8], extends the traditional HMM [18] in a hierarchic manner to include a hierarchy of hidden states. Each state in the normal HMM is generalized recursively as another sub-HMM with special *end* states included to signal when the control of the activation is returned to the parent HMM. The original HHMM in [8], however, requires a strict tree-like structure in the topological specification and thus limits its expressiveness and hinders its applications. This problem has been tackled recently in [3], in which a generalized form of the HHMM is introduced whose

topology can be a general lattice structure. More important, the extended HHMM can model shared structures that naturally exist in the domain. Because of the space restriction, we outline this model in the next section and refer readers to [3] for further details.

2.1 HHMM: Model definition

A discrete HHMM is formally defined by a 3-tuple $<\zeta,\mathcal{Y},\theta>:$ a topological structure ζ , an observation alphabet \mathcal{Y} , and a set of parameters θ . The topology ζ specifies the number of levels D, the state space at each level, and the parent-children relationship between levels d and d+1. The states at the lowest level (level D) are called *production* states. The states at a higher level d < D are termed *abstract* states. Only production states emit observation. Given a topological specification ζ and the observation space \mathcal{Y} , the set of parameters θ is defined as follows. Denote $B_{y|p}$ as the probability of observing $y \in \mathcal{Y}$ given that the production state is p. For each abstract state p^* at level d and the set of its children $ch(p^*)$, we denote π^{d,p^*} as the initial distribution over $ch(p^*)$, $A_{i,j}^{d,p^*}$ as the transition probability from child i to child i (i, i), i), and i0 as the probability that i1 the terminates given its current child is i1. The set of parameters i2 is i3 the structure of i4 the probability form i5. An abstract state i7 at level i8 and be executed as follows.

An abstract state p^* at level d can be executed as follows. First, p^* selects a state i at the lower level d+1 from the initial distribution π^{d,p^*} . Then, i is executed until it terminates. At this time, p^* can terminate with probability $A_{i,\text{end}}^{d,p^*}$. If p^* does not terminate, it continues to select a state j for execution from the distribution $A_{i,j}^{d,p^*}$. The loop continues until p^* terminates. The execution of p^* is similar to the execution of an abstract policy π^* in the AHMM [4], except that π^* selects a lower level policy π based only on the state at the bottom level, not on the policy π' selected in the previous step. However, the abstract state is a special case of the abstract policy in the AHMEM [2] (an extension of the AHMM).

A representation of the HHMM as a DBN is provided in [3], which defines a joint probability distribution (JPD) over the set of all variables $\{x_t^d, e_t^d, y_t \mid \forall (t,d)\}$, where x_t^d is the state at level d and time t, e_t^d represents whether x_t^d terminates or not, and y_t is the observation at time t.

2.2 Learning parameters in the HHMM

We need to learn the set of parameters θ of the HHMM from an observation sequence \mathcal{O} . Bui $et\ al.$ [3] have proposed a method based on the EM algorithm and the asymmetric inside-outside (AIO) algorithm to estimate θ . For this method, the set of hidden variables is $\mathcal{H}=\{x_t^d,e_t^d|t=1,\ldots,T,d=1,\ldots,D\}$, where T is the length of the observation sequence. The set of observed variables is $\mathcal{O}=\{y_1,\ldots,y_T\}$. Assume that τ is the sufficient statistic for θ . The EM algorithm reestimates θ by first calculating the expected sufficient statistic (ESS) $\bar{\tau}=\mathrm{E}_{\mathcal{H}|\mathcal{O}}\tau$. Then, the result is normalized to obtain the new value for θ . The ESS for the parameter $\mathrm{A}_{i,j}^{d,p^*}$, for example, is $\frac{\sum_{t=1}^{t=T-1} \xi_t^{d,p^*}(i,j)}{\mathrm{Pr}(\mathcal{O})}$,

where $\xi_t^{d,p^*}(i,j) = \Pr(x_t^d = p^*, x_t^{d+1} = i, x_{t+1}^{d+1} = j, e_t^d = F, e_t^{d+1} = T, \mathcal{O})$. The ESS for $A_{i,j}^{d,p^*}$ can be computed by the AIO algorithm [3]. The ESS for the other parameters of θ is computed in a similar manner. The complexity for the AIO algorithm is cubic in the length of the observation sequence, but linear in the number of states of the model.

2.3 Exact and approximate inference for the HHMM

The AIO algorithm can be used directly to derive an exact filtering algorithm as follows. At time t, $\xi_{t-1}^{d,p^*}(i,j)$ is computed by the AIO algorithm. Summing $\xi_{t-1}^{d,p^*}(i,j)$ over p^* , i, e_{t-1}^d and e_{t-1}^{d+1} , we obtain the probability $\Pr(x_t^{d+1}|y_1,\ldots,y_t)$. Note that, at the next time, $\xi_t^{d,p^*}(i,j)$ can be derived from $\xi_{t-1}^{d,p^*}(i,j)$ by stretching this probability one more time slice. Thus, the complexity of the exact filtering algorithm is $O(T^2)$. This algorithm can be well suited for short-term recognition, but it might not be realistic for a real-time recognition task when the observation length T grows. Alternatively, the RBPF has been successfully deployed in the AHMM [2] and can be readily adapted for the HHMM. Denote: $x_t^{1:D} \triangleq \{x_t^1,\ldots,x_t^D\}$, $e_t^{1:D} \triangleq \{e_t^1,\ldots,e_t^D\}$, $e_t^{1:D} \triangleq \{e_t^1,\ldots,e_t^{1:D}\}$, $y_{1:t} \triangleq \{y_1,\ldots,y_t\}$. The idea of the RBPF is that the filtering distribution at time t — that is, $\Pr(x_t^{1:D},e_t^{1:D}\mid y_{1:t})$ — is approximated via a two-step procedure: (1) sampling the Rao-Blackwellised (RB) variable $e_t^{1:D}$ from the current RB belief state $B_t = \Pr(x_t^{1:D},e_t^{1:D},y_t|e_{1:t-1}^{1:D})$, and (2) updating the RB belief state B_t using exact inference.

At each time step t, the algorithm maintains a set of N samples, each consisting of the distribution of one slice network $C_t \triangleq \Pr(x_t^{1:D} | e_{1:t-1}^{1:D})$. The RB belief state B_t can be obtained directly from C_t by adding in the network representing the conditional distribution of y_t and $e_t^{1:D}$. A new sample $e_t^{1:D}$ can be obtained from the canonical form of C_t (after obsorbing y_t). At the next time slice, C_{t+1} is constructed by projecting C_t over one slice based on the sampled value of $e_t^{1:D}$. The complete algorithm is shown in Algorithm 1. The complexity of the RBPF algorithm for the HHMM is O(ND), where N is the number of samples and D is the depth of the model.

3 Implementation

We apply the HHMM with shared structure to model people behaviors in a real environment. The environment is a room in which two static cameras are used to track people. We are interested in some special landmarks in the environment: the stove, cupboard, dining chair, fridge, TV chair, and door. Fig. 1(a) and (b) show the room and the special landmarks viewed from the two cameras. The room is divided into a grid of cells or states, which are numbered 1, 2,..., 24 (Fig. 2).

A two-level behavior hierarchy is defined in the environment. The top level consists of complex behaviors and the

Algorithm 1 RBPF for the HHMM

```
Begin For t=1,2,\ldots /* sampling step */
For each sample i=1,2,\ldots,N
Absorb y_t into C_t^{(i)}
Canonicalize C_t^{(i)}, update weight w_t^{(i)}=B_t(y_t)
Sample e_t^{1:D(i)} from C_t^{(i)} and \Pr(e_t^{1:D}\mid x_t^{1:D})
/* re-sampling step */
Normalize the weight \tilde{w}^{(i)}=\frac{w^{(i)}}{\sum_{i=1}^N w^{(i)}}
Re-sample the sample set according to \tilde{w}^{(i)}
/* exact step */
For each sample i=1,2,\ldots,N
Compute C_{t+1}^{(i)} from C_t^{(i)} and e_t^{1:D(i)}
/* Estimation step */
Compute \Pr(x_{t+1}^d\mid y_{1:t}) \approx \frac{1}{N} \sum_{i=1}^N C_{t+1}^{(i)}(x_{t+1}^d)
End
```

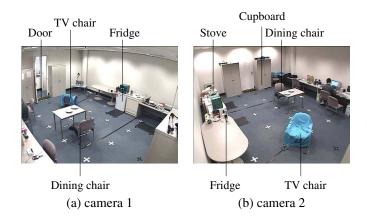


Figure 1. The scene viewed from the two cameras.

bottom level consists of primitive behaviors. A primitive behavior is a person's action of going from one landmark to another. The primitive behavior terminates when the person reaches the designated landmark. Table 1 shows 12 primitive behaviors defined in the environment.

A complex behavior is a person's action of visiting a sequence of landmarks. It can be refined into a sequence of primitive behaviors. We consider three complex behaviors — *short_meal*, *have_snack*, and *normal_meal* — of which the topologies are shown in Fig. 3(a), (b), and (c), respectively. Note that the topologies of these complex behaviors are specified by observing their typical patterns in the environment.

A person executing behavior *short_meal* will first enter the room via the door, go to the cupboard, and go to the fridge. Then, the person may exit the room via the door or go to the dining chair. From the dining chair, the person can exit the room or come back to the fridge. In the latter case, he again has two choices: exiting the room or going to the dining chair (Fig. 3(a)). The behavior *short_meal* involves the following landmarks: the door, cupboard, fridge, and dining chair. This complex behavior can be refined into a sequence of primitive

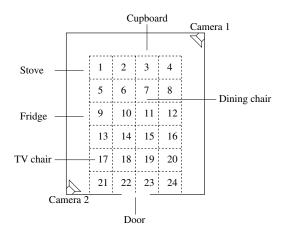


Figure 2. The environment used in the system.

Beh.	Landmarks	Beh.	Landmarks
1	Door→Cupboard	7	Fridge→TV chair
2	Cupboard→Fridge	8	TV chair→Door
3	Fridge→Dining chair	9	Fridge→Stove
4	Dining chair→Door	10	Stove→Dining chair
5	Door→TV chair	11	Fridge→Door
6	TV chair→Cupboard	12	Dining chair→Fridge

Table 1. The set of primitive behaviors.

behaviors 1, 2, 3, 4, 11, and 12.

The primitive and complex behaviors are mapped into a shared-structure HHMM, which has four levels. Level 1 is a root behavior. Levels 2 and 3 are the complex and primitive behaviors, respectively. Level 4 represents the states of the environment. Observations of these states are the cells in the environment. The hierarchy of behaviors and states is shown in Fig. 4. Note that some primitive behaviors are shared by multiple complex behaviors; for example, behavior 2 is shared by $short_meal, have_snack$, and $normal_meal$. The parameters of the HHMM are the matrices $\pi^{d,p}$, $A^{d,p}$, $A^{d,p}$ and the observation model B, where d=1,2, or 3 and p is a behavior at level d.

4 Experimental Results

4.1 Data and evaluations

The *training data* consists of 45 observation sequences obtained from 45 real scenarios. In each scenario, a person executes one of the three complex behaviors: *short_meal*, *have_snack*, and *normal_meal*. The person's trajectory is obtained from the tracking system, and converted into a sequence of cells or observations. As a result, we have 45 observation sequences. The *test data* is a different set of 43 observation sequences obtained in a similar way.

We evaluate the performance of different models in behavior recognition based on the *accuracy rate*, *early detection*, and *correct duration*. First, the *winning behavior* of an ob-

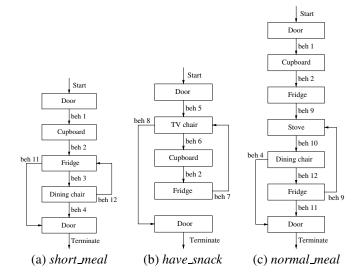


Figure 3. The complex behaviors.

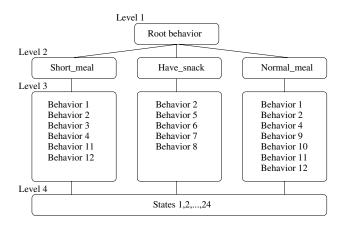


Figure 4. The behavior and state hierarchy.

servation sequence is defined as the complex behavior that is assigned the highest probability at the end of the sequence. Then, the accuracy rate is the ratio of the number of observation sequences, of which the winning behavior matches the ground truth, to the total number of test sequences. When the winning behavior matches the ground truth, we define: early detection $\triangleq \frac{t^*}{T}$, where T is the observation sequence length, and $t^* = min\{t | Pr(winning behavior) \text{ is highest}$ from time t to T. The early detection represents how early the system detects the winning behavior. We define: correct duration $\triangleq \frac{P}{T}$, where P is the total of the time period, in which the primitive behavior assigned the highest probability matches the ground truth. Note that the early detection and the correct duration refer to recognition performance at different levels in the hierarchy; they do not necessarily sum up to more (or less) than 100%. A reliable system in behavior recognition will have high accuracy rate, low early detection, and high correct duration.

4.2 Performance of hand-coded HHMM

The parameters of the hand-coded HHMM are initialized by observing typical patterns of the three complex behaviors short_meal, have_snack, and normal_meal. The exact filtering algorithm is used with the hand-coded HHMM to infer the behaviors at different levels. Fig. 5(a) shows the probability distribution of the complex behaviors for an observation sequence over time. From time $t^* = 25$ to the end of the sequence, normal_meal is being assigned the highest probability. Thus, normal_meal is the winning behavior of this sequence and the early detection is $t^*/T = 25/52 \approx 48.08\%$. We consider the results of querying the primitive behavior. The ground truth for this observation sequence is that a person executes primitive behaviors 1, 2, 9, 10, and 4 consecutively, with the corresponding starting times 1, 13, 25, 27, and 36, respectively. Fig. 5(b) shows the probabilities that the system assigns the primitive behaviors over time (behaviors with insignificant probability are omitted from the figure). The correct duration is approximately 94.23%, meaning that most of time the system detects the primitive behavior correctly.

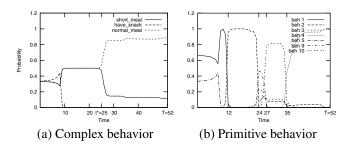


Figure 5. Querying the behaviors with the hand-coded HHMM.

Considering the results of querying the behaviors in the test data, which consists of 43 test sequences, the system recognizes correctly the *winning behavior* in 41 sequences. The accuracy rate is $41/43 \approx 95.35\%$. The averages of the early detection and correct duration are 52.90% and 66.72%, respectively.

4.3 Comparing learned HHMM with hand-coded HHMM, flat HMM, and tree HHMM

Compare against hand-coded HHMM. We learn the parameters of the HHMM using the EM and AIO algorithms [3] to obtain the learned HHMM. The training data is provided in Section 4.1. The learned HHMM is then used to recognize the behaviors in the 43 test sequences. Table 2 shows the performance of the learned HHMM in comparison with the hand-coded HHMM. The *accuracy rate* of the learned HHMM is higher than that of the hand-coded HHMM (100% versus 95.35%). The *early detection* of the learned HHMM is lower than that of the hand-coded HHMM is able to detect the *winning behavior* earlier. The *correct duration* of the learned HHMM is also higher than that of the hand-coded HHMM. The results show that the learned HHMM outperforms the hand-coded HHMM in behavior recognition.

	Learned HHMM	Hand- coded HHMM	Flat HMMs	Tree HHMM
Accuracy rate	100%	95.35%	90.70%	100%
Early detection	16.96%	52.90%	27.96%	31.74%
Correct duration	73.44%	66.72%		49.21%

Table 2. Performance of the learned HHMM, hand-coded HHMM, flat HMM and tree HHMM.

Compare against flat HMM. We use the flat HMM to recognize complex behavior. An HMM is created for each complex behavior *short_meal*, *have_snack*, or *normal_meal*. The parameters of an HMM are learned using the training data in Section 4.1. Table 2 compares the performance of the flat HMM with the learned HHMM. The same test data in Section 4.1 is used to evaluate the two models. The *accuracy rate* of the system with the flat HMM is lower than that of the system with the learned HHMM (90.70% versus 100%). The average of the *early detection* of the system with the flat HMM is 27.96%, which is higher than that of the system with the learned HHMM (16.96%). The results show that the learned HHMM is able to recognize the complex behaviors more accurately and earlier than the flat HMM.

Compare against tree HHMM. We create a tree HHMM from the shared-structure HHMM defined in Section 3 by duplicating each primitive behavior being the child of two complex behaviors (Fig. 6). The parameters for the tree HHMM are estimated using the EM algorithm with the training data provided in Section 4.1. The averaged time per one iteration in the case of the tree HHMM is about 1.5 times slower than that of the shared-structure HHMM. We use the tree HHMM to recognize behaviors in the 43 test sequences. The results in Table 2 show that the shared-structure HHMM recognizes the behaviors more reliably than the tree HHMM.

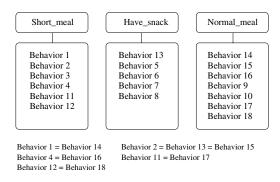


Figure 6. The primitive and complex behaviors of the tree HHMM.

4.4 Comparing the exact filtering algorithm with the RBPF

So far in this section, we have used the exact filtering algorithm based on the AIO method for behavior recognition. The computational complexity of this algorithm is $O(T^2)$. Thus, it is not realistic in long scenarios. Alternatively, we can use

the RBPF as discussed in Section 2 for the inference task. Table 3 compares the results of querying the behaviors using the RBPF and exact filtering algorithm. The test data described in Section 4.1 is used. When the number of samples N=50, the RBPF misclassifies the complex behavor in a test observation sequence. The accuracy rate is $42/43 \approx 97.67\%$. But when N=200, the RBPF detects correctly the complex behaviors in all test sequences (the accuracy rate is 100%). The early detection and correct duration obtained by the RBPF are about the same as the results obtained by the exact filtering algorithm (Table 3).

Fig. 7 compares the running time of the RBPF with the exact filtering algorithm. The running time for each time t of the RBPF is nearly constant, while that of the exact filtering algorithm increases significantly when t increases. As in the figure, when N=50 and 200, the running time of the RBPF is less than that of the exact filtering algorithm from time $t_1 = 3$ and $t_2 = 10$, respectively. At the end of the observation sequence (t=52), the RBPF is much faster than the exact filtering algorithm.

	Exact filtering	RBPF	
		N = 50	N = 200
Accuracy rate	100%	97.67%	100%
Early detection	16.96%	14.74%	15.97%
Correct duration	73.44%	73.45%	72.88%

Table 3. Comparing the performance of the exact filtering algorithm with the RBPF algorithm.

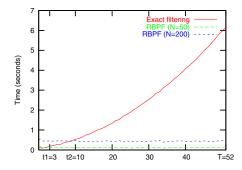


Figure 7. The running time for each time stamp of the exact inference and RBPF algorithms.

Conclusion

We have presented the use of the shared-structure HHMM to recognize people behaviors. The parameters of the HHMM have been learned from real and unlabeled data. We have used both the exact approximate inference algorithm and the RBPF to infer behaviors at different levels. Experimental results in a real environment demonstrate the ability of the sharedstructure HHMM to track people behaviors reliably, and the superiority of the shared-structure HHMM over the flat HMM and tree HHMM. The results also show the advantages of the RBPF inference algorithm to an exact method in a real application.

Acknowledgement

Hung Bui is supported by the Defense Advanced Research Projects Agency (DARPA), through the Department of the Interior, NBC, Acquisition Services Division, under Contract No. NBCHD030010.

References

- [1] D. Ayers and M. Shah. Monitoring human behavior from video taken in an office environment. *Image and Vision Computing*, 9(12):833–846, October 2001.
- [2] H. H. Bui. A general model for online probabilistic plan recognition. In Proceedings of the Eighteenth International Joint
- Conference on Artificial Intelligence (IJCAI-03), 2003.
 [3] H. H. Bui, D. Q. Phung, and S. Venkatesh. Hierarchical hidden Markov models with general state hierarchy. In Proceedings of the Nineteenth National Conference on Artificial Intelligence,
- pages 324–329, San Jose, California, 2004.
 [4] H. H. Bui, S. Venkatesh, and G. West. Policy recognition in the abstract hidden Markov model. Journal of Artficial Intelli-
- gence Research, 17:451–499, 2002. G. Cielniak, M. Bennewitz, and W. Burgard. Where is ...? Learning and utilizing motion patterns of persons with mobile robots. In Eighteenth International Joint Conference on Artificial Intelligence (IJCAI), pages 909-914, Acapulco, Mexico,
- [6] R. Collins, A. Lipton, T. Kanade, H. Fujiyoshi, D. Duggins, Y. Tsin, D. Tolliver, N. Enomoto, and O. Hasegawa. A System for Video Surveillance and Monitoring. Technical Report CMU-RI-TR-00-12, Robotics Institute, Carnegie Mellon Uni-
- versity, May 2000. A. Doucet, N. de Freitas, K. Murphy, and S. Russell. Rao-Blackwellised particle filtering for dynamic Bayesian networks. In Proceedings of the Sixteenth Annual Conference
- on Uncertainty in Artificial Intelligence, 2000. S. Fine, Y. Singer, and N. Tishby. The hierarchical hidden Markov model: Analysis and applications. *Machine Learning*, 32(1):41–62, 1998. A. Galata, N. Johnson, and D. Hogg. Learning variable length
- Markov models of behaviour. Computer Vision and Image Understanding Journal, 81:398–413, 2001. E. Grimson. VSAM.
- URL:
- http://www.ai.mit.edu/projects/darpa/vsam, 1998.
 [11] Y. Ivanov and A. Bobick. Recognition of visual activities and interactions by stochastic parsing. IEEE Transactions on Pattern Recognition and Machine Intelligence, 22(8):852-872,
- August 2000. [12] L. Liao, D. Fox, and H. Kautz. Learning and inferring transportation routines. *Proceedings of the National Conference on Artificial Intelligence(AAAI-04)*, 2004.
 [13] N. T. Nguyen, H. H. Bui, S. Venkatesh, and G. West. Recog-
- nising and monitoring high-level behaviours in complex spatial environments. In IEEE Conference on Computer Vision
- and Pattern Recognition, 2003.

 N. Oliver, E. Horvitz, and A. Garg. Layered representations for human activity recognition. In Fourth IEEE International Conference on Multimodal Interfaces, pages 3-8, Octo-
- ber 2002. [15] N. M. Oliver, B. Rosario, and A. Pentland. A Bayesian computer vision system for modeling human interactions. IEEE Transactions on Pattern Analysis and Machine Intelligence,
- 22(8):831–843, 2000. [16] S. Osentoski, V. Manfredi, and S. Mahadevan. Learning hierarchical models of activity. IEEE/RSJ International Confer-
- ence on Robots and Systems (IROS), to appear, 2004. [17] D. V. Pynadath and M. P. Wellman. Generalized D. V. Pynadath and M. P. Wellman. Generalized queries on probabilistic context-free grammars. *IEEE Transactions on Pattern Analysis and Machine Intelligence*, 20(1):65–77,
- [18] L. R. Rabiner. A tutorial on hidden Markov models and selected applications in speech recognition. *Proceedings of the IEEE*, 77(2):257–286, February 1989.

 [19] G. Wei and M. Tanner. A Monte-Carlo implementation of
- the EM algorithm and the poor man's data augmentation algorithms. Journal of the American Statistical Association, 85:699–704, 1990.